Injection Locking and Synchronization of Periodic and Chaotic Signals in Semiconductor Lasers

Y. Liu[1], P. Davis[1], Y. Takiguchi[1,2], T. Aida[1], S. Saito[1], J.M. Liu[3]

1 ATR Adaptive Communications Research Laboratories, 2-2 Hikaridai, Seika-cho, Soraku-gun, Kyoto 619-0288, Japan

2 Graduate School of Electronic Science, Shizuoka University, 3-5-1 Johoku, Hamamatsu, 432-8561 Japan

3 Department of Electrical Engineering, University of California at Los Angeles, Los Angeles, CA 90095 USA

Abstract

We experimentally investigate the synchronous response of a semiconductor laser to the injection of a periodic or chaotic oscillating optical signal that is generated by a similar semiconductor laser with optical feedback. We show that there are two different types of synchronous response, appearing in separate regimes of laser frequency detuning and injection strength. They are distinguished by the time lag of the slave laser response with respect to the

injection signal from output of the master laser. The experimental observations are well described by a numerical model consisting of a set of rate equations. It is revealed that the first type synchronous response corresponds to the synchronization solution of the equations and the second type of response is the result of strong injection. The relevance of these two types of synchronous behavior to a number of recent experiments on chaos synchronization and their implications on data encoding/recovery using chaotic carrier are discussed.

I. Introduction

Optical injection is a long studied technique related to all-optical communications and signal generation [1-4]. Injection locking where the oscillation in the slave laser is locked to a stable master signal, has been applied, for example, to stabilization of lasers, wavelength conversion, improvement of coherence, reduction of noise and enhancement of modulation bandwidth [5-7]. However, the dynamical behavior of a slave laser under a time varying injection signal can be complicated and has been less well studied or understood.

In this paper we look explicitly at this issue in the particular case of semiconductor lasers, which are key devices for possible applications of high-speed optical communications. In semiconductor lasers, complex oscillations can be easily induced by optical feedback or self-injection. Such oscillations have been extensively modeled by including a delayed feedback

term in laser models [8,9]. We consider a master laser with periodic or chaotic self-oscillations induced by optical feedback, and inject the oscillating master signal into a slave laser that has a similar free-oscillating frequency. We demonstrate that there are two different types of synchronous responses in the slave laser output. These can be easily distinguished experimentally by the difference in the time lag with respect to the injection signal. We show that in this particular scheme, these two types of synchronous responses occur in two different regimes characterized by weak injection and strong injection, respectively. In the weak injection regime, when the strength of the injection into the slave matches the strength of the feedback into the master, the slave laser reproduces the dynamics of the master laser induced by the external optical feedback and a complete synchronization state between the slave and master laser dynamics is achieved. Meanwhile, when the injection strength is much stronger than the feedback strength, a second type of synchronization between the output and input signals of the slave laser is observed. Such synchronous response is rather a driven response, and is distinguished by being synchronous with the injection signal rather than with the oscillation in the master laser.

Recently, optical injection has been enthusiastically studied as a means for realizing synchronization of chaotic oscillations in lasers, with possible applications in data communications [10-26]. Although synchronization of chaos has also been investigated in

electrical circuits [10] and opto-electric hybrid systems [12-15], synchronization of chaotic oscillations in lasers differs from synchronization of chaos in electrical circuits in the aspect that it involves locking of optical carrier as well as synchronization of slower modulations of the amplitude and phase [16-26]. It will be important to distinguish the two different types of synchronous responses from viewpoints of both fundamental research of semiconductor lasers and applications of lasers to communications. In this paper, we will discuss how our observations of two types of synchronous responses are related to recent experiments on chaos synchronization as well as data communication schemes using chaos.

This paper is organized as follows. In the next section, we describe the setup of the experimental system. In Section III, we show experimental results on the synchronous responses to periodic and chaotic injection light from the master laser. Two types of synchronization states are observed at different injection regimes: The first type occurs when the injection strength matches the feedback level, while the second type occurs when the former is much stronger than the latter. The difference between the two synchronization states is investigated via the dependence on the detuning frequency and the time lag with respect to the injection signal. In Section IV, we conduct numerical calculations using two sets of rate equations which describe the laser with external optical feedback and the laser with optical injection, respectively. Using laser parameter values estimated from the experiments, we successfully reproduced

experimental observations. In Section V, we discuss the relevance between our work and recent studies on laser chaos synchronization and optical communications using chaotic carrier. We summarize our results in Section VI.

II. Experimental Setup

The experimental system consists of two laser diodes coupled in the configuration shown in Fig. 1. We use two similar single-mode DFB laser diodes (NEL-NLK1555) driven with a low-noise high-precision controller stabilizing the injection current and the temperature to within 0.01 mA and 0.01 K, respectively. At the temperature of 24.0°C, the threshold injection current I_{th} of the free-running laser is 7.6 mA. At the injection current I_b=11.4 mA (~ 1.5 I_{th}), the oscillating laser wavelength is 1537.17 nm with a linewidth of about 4 MHz. The dependencies of the laser wavelength on the temperature and the injection current are measured to be 0.106 nm/K (12.46 GHz/K) and 0.004 nm/mA (500 MHz/mA), respectively. The frequency detuning between the two lasers at the free-running state is fine-tuned by varying the injection current and the temperature, allowing matching of the optical frequencies of the two lasers to within 10 MHz. The lasing wavelength is monitored with an optical spectrum analyzer (HP71450A, 0.1 nm resolution). The intensity variations of the laser outputs are detected by 6 GHz bandwidth photoreceivers (New Focus 1514LF) and observed on a digital oscilloscope

(Tektronix TDS694C) with a 3 GHz bandwidth and a 10 Gbps sampling rate as well as on an RF spectral analyzer (Advantest R3267) with an 8 GHz bandwidth.

The light output from the right facet (high-reflection (HR) coated, reflection >95%) of the master laser is fed back to the left facet (anti-reflection (AR) coated, reflection <1%) of the master laser. The light output from the AR-coated facet of the master laser is injected to the slave laser on the AR coated facet so that a strong injection strength can be achieved. A 60 dB optical isolator is inserted in each of the feedback and the injection paths to avoid multiple reflections in the external cavity of the master laser and to ensure unidirectional coupling from the master to the slave laser. Half-wave plates (HWPs) are used to adjust the polarization states of the feedback/injection light in order to obtain the maximum feedback/injection effects. Unless otherwise noted, the time delay of the external ring cavity, t, and the transmission time between the master and the slave lasers, t_c, are fixed at 3.3 and 5 ns, respectively. The feedback level, as well as the injection strength, is varied with neutral density filters.

For the master laser, the external optical feedback induces a variety of rich and complex dynamics as have been investigated in many previous works [8,9]. A main difference between the current external ring cavity and the optical feedback from an external mirror as employed in many previous external-cavity laser diode experiments [8,9,24-26] is that the effect of multiple reflection is completely avoided in the current experiment due to the unidirectional external ring

configuration. Since one facet of the laser diode used in our experiments has a HR coating, the feedback light level is limited to a relatively low level (P_{ext}<20 μW). This feedback level is strong enough to induce unstable intensity variations such as periodic oscillations and chaos in the light output of the master laser. The laser spectrum shows that, even when the laser output is chaotic, the side-mode suppression ratios of both lasers are measured to be about 40 dB, which guarantees the single-mode operation of both lasers.

III. Experimental Results

We experimentally investigate the dynamics of the slave laser subject to different types of optical injection signals. In particular, we focus on how the slave laser responds to the injection signal when the injection power is continuously varied.

A. Synchronization of Periodic Signals

We start from the investigation of the response of the slave laser to the injection of a periodic oscillation. Trace A in Fig. 2 depicts a periodic injection signal generated by the master laser at I_b=11.4 mA, t=3.3 ns, and P_{ext}=2 μW. Traces B-D show typical types of the slave laser output signals obtained at different injection conditions. The optical frequencies of the two lasers are matched to within 10 MHz. All traces in Fig. 2 are plot with the same scale. Trace B in Fig. 2 shows the slave laser output at the injection power close to the feedback power, i.e.,

$P_{inj} \approx P_{ext}$. Here, P_{inj} is the averaged injection power measured into the slave laser. At this condition $P_{inj} \approx P_{ext}$, the slave laser output shows an almost identical waveform to the injection signal. Trace C in Fig. 2 shows the slave laser output at a much stronger injection power $P_{inj} \approx 100P_{ext}$. The slave laser shows a totally different behavior from the master laser. One observes a chaotic waveform with the average frequency (~4.8 GHz) much higher than the frequency of the periodic injection signal (~3.2 GHz). When we further increase the injection power, the waveform of the slave laser becomes synchronous with the injection signal again. Trace D in Fig. 2 shows the slave output at $P_{inj} \approx 400P_{ext}$. One obtains a periodic signal with the period exactly the same with the injection signal. The waveform of the slave laser output at strong injection is, however, different from that at weak injection in two aspects. First, the amplitude of the former is larger due to the strong injection. Second, the phase difference (time lag) of the slave laser output with respect to the injection signal is different between these two cases. This is a particularly important characteristic of synchronization that will be further discussed laser.

The response of the slave laser to the periodic injection signal is systematically illustrated in Fig. 3 by a bifurcation diagram that is obtained by sampling the slave laser output time series at the period of the injection signal. Here, the injection strength is denoted as the square root of the injection light power. In general, a synchronized periodic oscillation is

denoted by a single spot on the bifurcation diagram. However, due to effects of noise and sampling error, such spot might be 'diffused' to a certain degree as seen in Fig. 3. From Fig. 3, it is found that the slave laser shows synchronized periodic oscillations in (I) a weak injection regime where $P_{inj} \approx P_{ext}$ and (II) a very strong injection regime where $P_{inj} >> P_{ext}$. For the injection strength between these two regions, the slave laser output shows totally different waveforms from the master laser as shown in trace C of Fig. 2.

B. Synchronization of Chaotic Signals

Next, we move on the response of the slave laser to a chaotic injection signal. By increasing the feedback power in the master laser, we observed a continuous bifurcation in the master laser output spanning from periodic oscillations to chaos. Here, we show how the slave laser responds to a specific chaotic signal generated by the master laser at I_b=11.4 mA, t=3.3 ns, and P_{ext}=4 μW. We found that, similar to the case of periodic injection signal, there are three types of qualitatively different responses in the slave laser output corresponding to different injection conditions. Figure 4(a) shows the output waveforms of the master and slave lasers at $P_{inj} \approx P_{ext}$. An excellent synchronization between the slave and master laser outputs is verified from the times series and as well as the radio-frequency (RF) power spectra which are not shown here. Figure 4(b) shows the laser outputs obtained at $P_{inj} \approx 10P_{ext}$. At this condition, the

slave laser output greatly differs from that of the master laser at both the waveform and the average frequency. Figure 4(c) shows the laser outputs obtained at $P_{inj} \approx 100 P_{ext}$. Once again, the slave laser shows similar waveform to that of the master laser output.

For a chaotic injection signal, we define a correlation function r in the following to give a direct measure of the similarity between the master laser and the slave laser output signals.

$$r = \mathrm{MAX}\left\{ \frac{\mathrm{Cov}(x^M, x^S; \Delta)}{s_{x^M} s_{x^S}} \right\}\Bigg|_{\Delta}, \tag{1}$$

where $x^M \sim \left|E^M\right|^2$, $x^S \sim \left|E^S\right|^2$, $s_x^2 = \frac{1}{T}\int_0^T \left(x(t) - \bar{x}\right)^2 dt$,

$\mathrm{Cov}(x, y; \Delta) = \frac{1}{T}\int_0^T \left(x(t) - \bar{x}\right)\left(y(t+\Delta) - \bar{y}\right) dt$, and $\bar{x}$ denotes the time average of $x(t)$. Figure 5 shows the variation of r as a function of $(P_{inj})^{1/2}$. One easily finds that, like the case of periodic oscillations, there are two separate injection regimes, i.e., regime I around $P_{inj} \approx P_{ext}$ and regime II at $P_{in} >> P_{ext}$, where a high correlation between the master and slave laser outputs is achieved. In regime I, the correlation shows a very sensitive dependence on the injection strength; while in regime II, the correlation approaches a high level after the injection strength exceeds a certain point.

C. Time Lag between the Synchronized Slave Laser and the Master Laser

In both of the above synchronization regimes, there exists a time lag between the output of the slave and master laser outputs. The time lag T_d is explicitly defined in Eq. (1) as the value of D for which the correlation function r reaches the maximum. For the time series obtained at P_{inj}=P_{ext} (Fig. 4(a)) in regime I, r is calculated to be 0.9 and the synchronization time lag T_d is 1.7 ns, which is equal to the value t_c-t. For the time series obtained at P_{inj}=100P_{ext} (Fig. 4(c)) in regime II, the value of r is calculated to be 0.88 and the time lag T_d is 5.0 ns, which is equal to the value t_c. In Fig. 5, the time lag T_d abruptly jumps from t_c-t to t_c at a certain injection strength C, where the value of r reaches the minimum. To confirm the difference between the two synchronized scenarios, we experimentally measure the dependence of the time lag T_d on the delay time t. Figure 6 shows the variation of T_d as a function of the delay time t for the case of chaotic injection. Clearly, for the first type of synchronous response observed at regime I, we obtain the relationship T_d=t_c-t; while for the second type of synchronous response at regime II, we obtain T_d=t_c. For periodic injection signals, we also observed different time lags at the two different synchronization regimes. The only exception is that the observed time lag at periodic injection signals was T_d mod T_p where T_p is the period of the injection signal. Hereafter, we refer to the synchronization state where T_d =t_c-t can be identified as type I synchronization, and the synchronization state where T_d=t_c is identified as type II synchronization.

The difference in the time lag is essential to distinguish the two types of

synchronization states. Assuming a special case $t_c=t$, the type I synchronization implies that the output of the slave laser, $E^S(t)$, reproduces the output of the master laser, i.e., $E^S(t)=E^M(t)$, while receiving the injection signal $E^M(t-t_c)$ from the master laser; whereas the type II synchronization implies that the slave laser in a sense becomes transparent to the injection signal, i.e., $E^S(t)\propto E^M(t-t_c)$, due to strong driving by the injection signal.

D. Effects of Detuning Frequency

The difference between the two types of synchronization states is manifested also in terms of the dependence of the synchronization quality on injection strength and frequency detuning. Figure 5 demonstrated that the dependence of the correlation function on the injection strength is much more sensitive at regime I than at regime II. The effect of the detuning frequency between two lasers shows even larger difference between the two synchronization regimes. Here, we only describe the results on chaotic injection signals. Similar results have been obtained for periodic injection signals. Figure 7 shows the correlation function r as a function of the detuning frequency for (a) type I and (b) type II synchronization cases. For type I synchronization, r has a maximum value at W=0 and shows a dramatic decrease as W deviates from 0. The frequency range for stable injection locking with a constant injection light power P_{inj}=4 μW is measured to be -1.8 GHz < $W/2\pi$ < -0.35 GHz. We note that this stable injection

locking range does *not* coincide with the frequency detuning range where good chaos synchronization performance is achieved. For type II synchronization, however, high synchronization quality is achieved over a wide frequency detuning range as shown in Fig. 7(b). The stable injection locking frequency range at P_{inj}=500 μW is measured to be -12.8 GHz < $W/2\pi$ < 0.7 GHz which is close to the synchronization range. This shows that good type II chaos synchronization performance is achieved over the frequency range where stable injection locking occurs. Around the lower boundary of the stable injection locking range, we observed intermittency between two types of oscillations, i.e., synchronized oscillations (Fig. 4(a)) and desynchronized oscillations (Fig. 4(b)). Such intermittency results in a tremendous collapse of the correlation function near the lower boundary in Fig. 7(b). We do not observe such fluctuations at the upper boundary of the stable injection range.

IV. Numerical Results

The dynamical behavior of the lasers in our experimental scheme can be modeled by two equations describing the complex electric fields of the master laser, E^M, and the slave laser, E^S, respectively [22, 23, 27].

$$\frac{dE^M(t)}{dt} = -\frac{g_c}{2}E^M(t) + j(w_0 - w_c)E^M(t) + \frac{\Gamma}{2}(1 - ja)g^M E^M(t) + h_{ext}E^M(t - t)\exp(iw_0 t), \tag{2}$$

$$\frac{dE^S(t)}{dt} = -\frac{g_c}{2}E^S(t) + j(w_0 - w_c + \Omega)E^S(t) + \frac{\Gamma}{2}(1 - ja)g^S E^S(t) + h_{inj}E^M(t - t_c)\exp(iw_0 t_c)\,. \tag{3}$$

Here, the superscripts M and S denote master and slave lasers, respectively, N represents the carrier density in the laser active layer, g_c is the cavity decay rate, w_0 is the master laser frequency, w_c is the longitudinal mode frequency of the cold laser cavity, W is the detuning frequency between the master and slave lasers, G is the confinement factor, a is the linewidth enhancement factor, and g is the gain coefficient. The gain coefficient is further assumed to obey a linear dependence on changes in the carrier density N and changes in the photon density S in the form $g = g_c/\Gamma + g_n(N - N_0)/S_0 + g_p(S - S_0)/\Gamma S_0$, where N_0 and S_0 are respectively nominal carrier density and photon density at the operation point and g_n and g_p are relaxation rates contributed respectively by the differential and nonlinear gain parameters of the laser [27]. The first equation describes the dynamics of a semiconductor laser with optical feedback with the feedback strength h_{ext} and the round trip time t. The second equation describes the dynamics of a semiconductor laser with optical injection from the master laser with the injection strength h_{inj} and the propagation time t_c. The carrier density within the cavity is further described by the following equation:

$$\frac{dN^{M,S}(t)}{dt} = \frac{J}{ed} - g_s N^{M,S}(t) - \frac{2e_0 n^2}{\hbar w^{M,S}} g^{M,S}\left|E^{M,S}(t)\right|^2, \tag{4}$$

where J is the injection current density, e is the electronic charge, d is the active layer thickness,

g_s is the carrier decay rate, e_0 is the permitivity of the free space, and n is the effective refractive index of the semiconductor structure for the laser mode.

One can easily find that an identical synchronization solution, $E^S(t)=E^M(t-t_c+t)$, exists in the above equations when $h_{inj}=h_{ext}$ and $W=0$. It can also be shown that this is a stable solution, i.e, an attracting solution, in certain parameter conditions [21-23]. Note that there exists a time lag $T_d=t_c-t$ between the slave and master lasers for this identical synchronization solution. Such analytical solution corresponds to what we have experimentally observed around $P_{inj}=P_{ext}$ in regime I. For this reason, we also referred to the type I synchronization state as the complete synchronization. On the other hand, for large injection strength, $h_{inj}>>h_{ext}$, although identical synchronization solution does not exist due to the lack of symmetry between Eq. (2) and Eq. (3), the slave laser is strongly driven by the injection signal and we might expect the slave laser output to follow the oscillations of the injection signal. A previous numerical study [21,22] showed such a synchronous behavior persists at strong injection. It was also shown that, when the slave laser is subject to a strong injection signal, the time lag is determined only by the propagation time, i.e., $T_d=t_c$. Though very similar optical and RF spectra between the two lasers may be observed in both cases, the time lag manifests the difference between the two scenarios.

To reproduce the experimental results, we numerically integrate equations (2)~(4) and calculate the response behavior of the slave laser to both periodic and chaotic injection signals

generated by the master laser with external optical feedback. The parameters for the numerical model are estimated using a laser parameter characterization method based on optical injection [27]. Details are left to Appendix A. The values of the key parameters of the DFB semiconductor laser used in current experiments are g_c=1.4×10^{11} s^{-1}, g_s=3.37×10^9 s^{-1}, g_n=3.11×10^9 s^{-1}, g_p=2.7×10^9 s^{-1}, a=3.5, G=0.4 at I_b=1.5I_{th}. Figure 8 shows the bifurcation diagram of the slave laser output (obtained by sampling the times series at the period of the injection signal) to a periodic injection generated by the master laser at I_b=1.5I_{th}, t=3.3 ns, and h_{ext}=1.85×10^9 s^{-1}. Here the injection strength is normalized to the feedback strength as h_{inj}/h_{ext}. One observes synchronized periodic oscillations (denoted as single dots) at either weak injection regime ($h_{inj}\approx h_{ext}$) or strong injection regime ($h_{inj}>>h_{ext}$). Between regimes I and II, the slave laser output exhibits chaotic oscillations showing completely different amplitude and frequency with the injection signal. Figure 9 shows the correlation function r as a function of the injection strength at a chaotic injection signal generated by the master laser at I_b=1.5I_{th}, t=3.3 ns, and h_{ext}=4.0×10^9 s^{-1}. Here again, the numerical results demonstrated the existence of two different injection regions where synchronization is observed. We also calculated the time lag T_d from the time series and investigated its dependence on the injection strength. We $T_d=t_c-t$ at regime I and to $T_d=t_c$ at regime II.

Dependencies of the synchronization performance on the frequency detuning are also

investigated numerically and the results for chaotic injection are plotted in Fig. 10 for (a) type I and (b) type II synchronization states. For type I synchronization, r shows a maximum value at W=0 and rapidly decreases as W deviates from 0. For type II synchronization, r stays rather constant over a wide range of the detuning frequencies. There is also a sudden collapse of the correlation function around the lower boundary of the stable injection locking range. These results are in full agreement with experimental observations.

V. Discussions

Because of the symmetry between Eq. (2) for the laser with external optical feedback and Eq. (3) for the laser with optical injection, the optical injection scheme shown in Fig. 1 is considered as an effective means to synchronize the chaos induced by optical feedback. A number of interesting experimental results have recently been achieved which show synchronization of chaotic signals at the frequency ranges of MHz to GHz [23-26]. It is worthwhile to discuss the relevance between our experiments and previous theoretical and experimental works. In our previous numerical work, we demonstrated that the type I synchronization state could only be stable at either relatively weak or very strong feedback levels [22]. In this experiment, we find that type I synchronization can be achieved when the feedback level is relatively low (P_{ext}<10 μW). At a moderate feedback level (10 μW<P_{ext}<20

μW), only type II synchronization was observed. Moreover, the type II synchronization state has a larger tolerance to parameter mismatches than the type I case. Therefore, it can be generally concluded that, for a chaotic/periodic injection signal that is generated by a weak to moderate optical feedback, type II synchronization is more easily observed in experiments than type I synchronization. On the other hand, the necessary injection power to achieve the type II synchronization state does not depend on the complexity of the injection signal. Comparing Fig. 3 with Fig. 5, we find that good synchronization quality can be obtained around the injection power P_{inj}≈225 μW for either periodic or chaotic injection signals. The same tendency is also observed in the numerical results shown in Figs. 8 and 9. One expects a more robust complete synchronization state (with more tolerance to parameter mismatches) when a strong feedback, strong injection condition, e.g., P_{inj}=P_{ext}>200 μW, is realized. Indeed, our previous numerical simulations [22] supported such conclusion. In the present experiment, the feedback level is limited by the laser configuration (AR-HR coating). A laser with a smaller facet reflectivity or with an external amplifier in the feedback loop can be used to implement such experiments.

Chaos synchronization has been applied to communication systems over a wide range of bandwidth [10-16]. Synchronization of optical-feedback-induced chaos is among the first schemes proposed for applying chaos synchronization to high-frequency communication systems. Here, we briefly discuss how the observed two types of synchronization states can be

applied to different communication schemes proposed so far. Several recent experiments employed a chaos masking scheme by superimposing a small modulated optical signal onto the injection light. Message decoding at the receiver end is conducted by taking the difference between the slave laser output signal and the injection light signal. Fischer et al. [26] reported that it is possible to mask a sinusoidal signal with a frequency larger than 1 GHz. Such chaos masking scheme can be implemented based on either type I or type II synchronization states. Experimentally, type II synchronization is more robust to noise and parameter mismatches. Recently, Liu et al. [23] applied a direct encoding scheme [11-13] to the optical feedback system. The main advantage of this method is that it does not require the encoded message to be at a lower frequency compared to the chaotic carrier signal. It was verified via numerical simulations that a pseudo-random signal at the bit rate of 2.5 Gbps was successfully transmitted and decoded using the proposed scheme. We note that such direct encoding scheme can only be implemented at type I synchronization regime.

VI. Conclusions

In conclusion, we have demonstrated that there are two types of synchronization states in a pair of laser diodes coupled by optical injection in a master-slave scheme. The first type is found when the frequency detuning is small and the injection strength matches the feedback

strength of the master laser. In this synchronization state, the slave laser reproduces the dynamics of the master laser as expected from the symmetry of the system. In the second type, found over a wide detuning range when the injection strength is much stronger than the feedback strength, the slave laser becomes in a sense a modulator for the injection signal. The two types of synchronization states have different properties in terms of the time lag between the output waveforms of the two lasers, the tolerance to parameter mismatch, and the relation to the stable injection locking range. The experimental observations are well described by a numerical model consisting of a set of rate equations. It is revealed that the first type of synchronization corresponds to the synchronization solution of the equations and the second type is the result of strong injection. Using parameters estimated from lasers, we have successfully reproduced experimental observations with numerical simulations. Our observation of two types of synchronous behavior well described the relevance between theoretical and experimental results on optical-feedback-induced chaos synchronizations reported so far. Two types of synchronization states can be applied to different schemes of optical communications using chaotic carrier.

Appendix A Parameter Characterization of the DFB Laser Used in the Experiments

We experimentally characterized the parameters of the DFB laser employed in our

experiments using a laser parameter characterization method based on the four-wave mixing technique described in Ref. [27].

The first step of parameter characterization is to experimentally measure two four-wave mixing spectra the laser of interest under weak optical injection: the regenerative reflectivity spectrum given in Eq. (30) of Ref. [27] and the power spectrum given in Eq. (31) of Ref. [27]. Figure A-1 shows a typical example of such experimental results measured at a certain laser injection current. The solid curves in the figure are theoretical fittings of the experimental data using Eqs. (30) and (31) of Ref. [27] with best fitting parameters. From data fitting, one can obtain values for parameters W_r, g_r, g_p, and a. The next step of parameter characterization is to repeat the above measurement at different injection current levels. This gives the laser power dependence of the measured parameters [27]. The results are summarized in Fig. A-2. These results give us the following linear dependencies: $f_r^2 = 3.09P - 0.18$ GHz^2, $g_r = g_s + g_n + g_p = 1.59P + 3.37$ s^{-1}, $g_p = 0.73P + 0.02$ s^{-1}, where P is the laser power in mW and f_r, g_r, and g_p have the unit of 10^9 s^{-1}. At the injection current I_b=1.5 I_{th}, the light power is measured to be P=3.64 mW. Using the above results, we obtain the following parameter values: f_r=3.34 GHz, W_r=20.98 GHz, g_r=9.05×10^9 s^{-1}, g_p=2.7×10^9 s^{-1}, a=3.5, $g_s = g_r(P=0) = 3.37\times10^9$ s^{-1}, $g_n = 0.86P \times10^9$ s^{-1}=3.11×10^9 s^{-1}, and

$g_c = \frac{\left(\Omega_r^2 - g_s g_p\right)}{g_n} = 1.40 \times 10^{11}\ \mathrm{s}^{-1}$ for the DFB laser used in our experiments.

Acknowledgments

We are grateful to Dr. B. Komiyama for encouragement and support. Y. Liu and Y. Takiguchi acknowledge helpful support by Prof. J. Ohtsubo.

References

[1] S. Kobayashi, Y. Yamamoto, and T. Kimura, "Optical FM signal amplification and FM noise-reduction in an injection locked AlGaAs semiconductor laser," *Electron. Lett.*, Vol. 17, pp. 849-851, 1981.

[2] S. Saito, F. Mogensen, and H. Olesen, "Effective bandwidth for FM noise suppression in an injection-locked semiconductor-laser," *Electron. Lett.*, Vol. 21, pp.1173-1175, 1985.

[3] A. Egan, M. Harley-Stead, P. Rees, S. Lynch, P. McEvoy, J. O'Gorman, and J. Hegarty, "All-optical synchronization of self-pulsating laser diodes," *Appl. Phys. Lett.*, Vol. 68, pp. 3534-3536, 1996.

[4] P. M. Varangis, A. Gavrielides, T. Erneux, V. Kovanis, and L. F. Lester, "Frequency entrainment in optically injected semiconductor lasers," *Phys. Rev. Lett.*, Vol. 78, pp.2353-2356, 1997.

[5] L. Goldberg and M. K. Chun, "Injection locking characteristics of a 1-W broad stripe laser diode," *Appl. Phys. Lett.*, Vol. 53, pp.1900-1902, 1988.

[6] J. Wang, M. K. Haldar, L. Li, and F. V. C. Mendis, "Enhancement of modulation bandwidth of laser diodes by injection locking," *IEEE Photonics Tech. Lett.*, Vol. 8, pp.34-36, 1996.

[7] T. B. Simpson and J. M. Liu, "Bandwidth enhancement and broadband noise reduction in injection-locked semiconductor lasers," *IEEE Photonics Tech. Lett.*, Vol. 9, pp.1322-1324, 1997.

[8] B. Tromborg, J. H. Osmundsen, and H. Olesen, "Stability analysis for a semiconductor laser in an external cavity," *IEEE J. Quantum Electron.*, Vol.20, pp. 1023-1032, 1984.

[9] J. Mørk, B. Tromborg, and J. Mark, "Chaos in semiconductor lasers with optical feedback – theory and experiment," *IEEE J. Quantum Electron.*, Vol. 28, pp.93-108, 1992.

[10] L. M. Pecora and T. L. Carroll, "Synchronization in chaotic systems," *Phys. Rev. Lett.*, Vol. 64, pp. 821-824, 1990.

[11] G. D. Van Wiggeren and R. Roy, "Communication with chaotic lasers," *Science*, Vol. 279, pp. 1198-1200, 1998.

[12] J. P. Goedgebuer, L. Larger, and H. Porte, "Optical cryptosystem based on synchronization of hyperchaos generated by a delayed feedback tunable laser diode," *Phys. Rev. Lett.*, Vol. 80, pp. 2249-2252, 1998.

[13] Y. Liu, P. Davis, and T. Aida, "Synchronized chaotic mode hopping in DBR lasers with delayed opto-electronic feedback," *IEEE J. Quantum Electron.*, vol. 37, pp. 337-352, 2001.

[14] P. Davis, Y. Liu, and T. Aida, "Chaotic wavelength-hopping device for multiwavelength optical communications," *IEEE Trans. C&S*, Vol. 48, pp. 1523-1527, 2001.

[15] A. Uchida, S. Yoshimori, M. Shinozuka, T. Ogawa, and F. Kannari, "Chaotic on-off keying for secure communications," *Opt. Lett*., Vol. 26, pp.866-868, 2001.

[16] J. M. Liu, H. F. Chen, and S. Tang, "Optical-communication systems based on chaos in semiconductor lasers," *IEEE Trans. C&S*, Vol. 48, pp. 1475-1483, 2001.

[17] P. Colet, and R. Roy, "Digital-communication with synchronized chaotic lasers," *Opt. Lett*., Vol. 19, pp.2056-2058, 1994.

[18] C. R. Mirasso, P. Colet, and P. Garcia-Fernandez, "Synchronization of chaotic semiconductor lasers: application to encoded communications," IEEE Photonics Tech. Lett., vol. 8, pp. 299-301, 1996.

[19] V. Annovazzi-Lodi, S. Donati, and A. Sciré, "Synchronization of chaotic lasers by optical feedback for cryptographic applications," IEEE J. Quantum Electron., vol. 33, pp. 1449-1454, 1997.

[20] J. K. White and J. V. Moloney, "Multichannel communiation using an infinite dimensional spatiotemporal chaotic system," *Phys. Rev. A*, vol. 59, pp. 2422-2426, 1999.

[21] V. Ahlers, U. Parlitz, and W. Lauterborn, "Hyperchaotic dynamics and synchronization of external-cavity semiconductor lasers," *Phys. Rev. E*, vol. 58, pp. 7208-7213, 1998.

[22] Y. Liu, H. F. Chen, J. M. Liu, P. Davis, and T. Aida, "Synchronization of optical-feedback-induced chaos in semiconductor lasers by optical injection," *Phys. Rev. A*, vol. 63, pp. 031802-1-4, 2000.

[23] Y. Liu, H. F. Chen, J. M. Liu, P. Davis, and T. Aida, "Communication using synchronization of optical-feedback-induced chaos in semiconductor lasers," *IEEE Trans. C&S*, Vol. 48, pp. 1484-1490, 2001.

[24] S. Sivaprakasam and K. Shore, "Demonstration of optical synchronization of chaotic external-cavity laser diodes," *Opt. Lett*., Vol. 24, pp. 466-468, 1999.

[25] Y. Takiguchi, H, Fujino, and J. Ohtsubo, "Experimental synchronization of chaotic oscillations in externally injected semiconductor lasers in low-frequency fluctuation regime," *Opt. Lett*., Vol. 24, pp.1570-1572, 1999.

[26] I. Fischer, Y. Liu, and P. Davis, "Synchronization of chaotic semiconductor laser dynamics on sub-ns timescales and its potential for chaos communication," *Phys. Rev. A*, Vol. 62, pp.

011801-1-4, 2000

[27] J. M. Liu and T. B. Simpson, “Four-wave mixing and optical modulation in a semiconductor laser,” *IEEE J. Quantum Electron*., Vol. 30, pp.957-965, 1994.

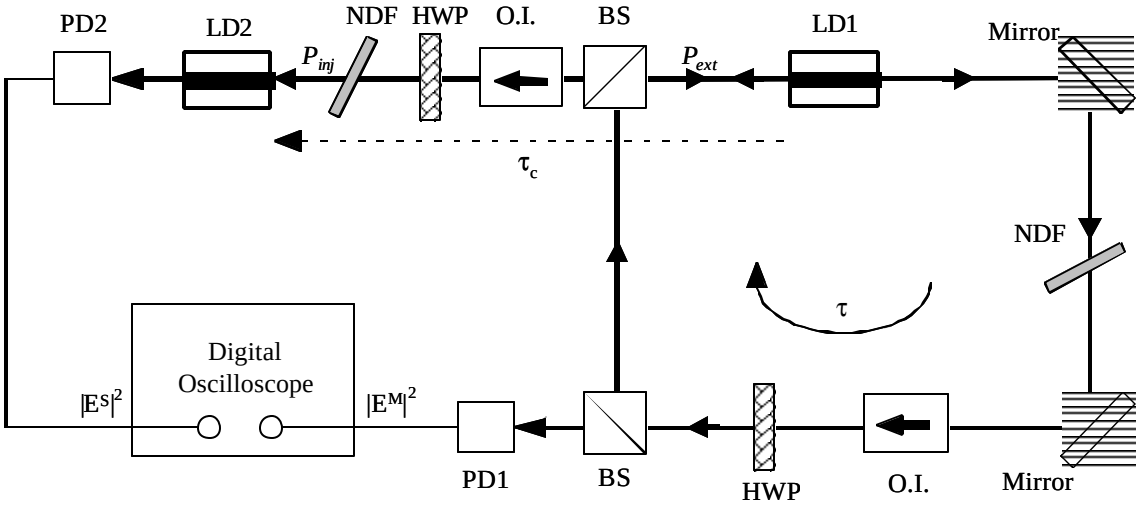

Fig.1 Experimental setup. LD1: master laser, LD2: slave laser, PD: photodiode, O.I.: optical isolator, BS: beam-splitter, HWP: half-wave plate, NDF: neutral density filter. P_{inj} (P_{ext}): injection (feedback) power into the slave (master) laser.

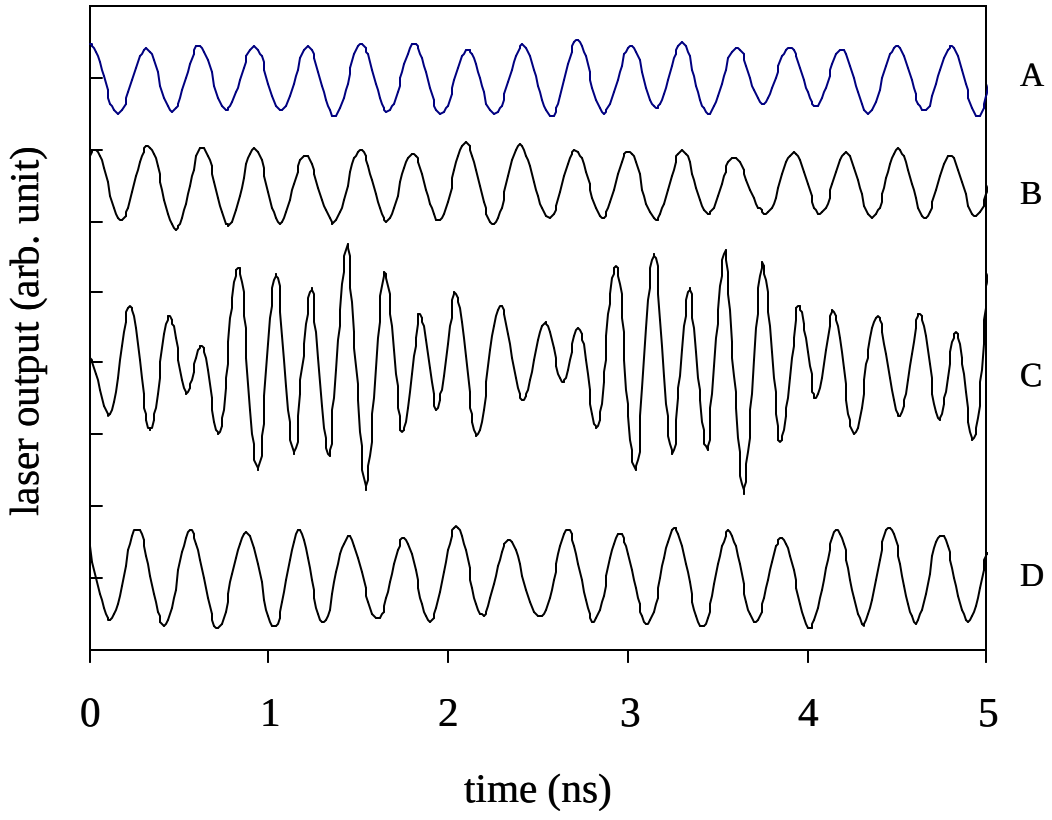

Fig.2 Slave laser outputs to periodic injection signal. Trace A: master laser output (injection) signal; trace B: slave laser output at $P_{inj} \approx P_{ext}$; Trace C: slave laser output at $P_{inj} \approx 100P_{ext}$; trace D: slave laser output at $P_{inj} \approx 400P_{ext}$. All traces are plot in same scale.

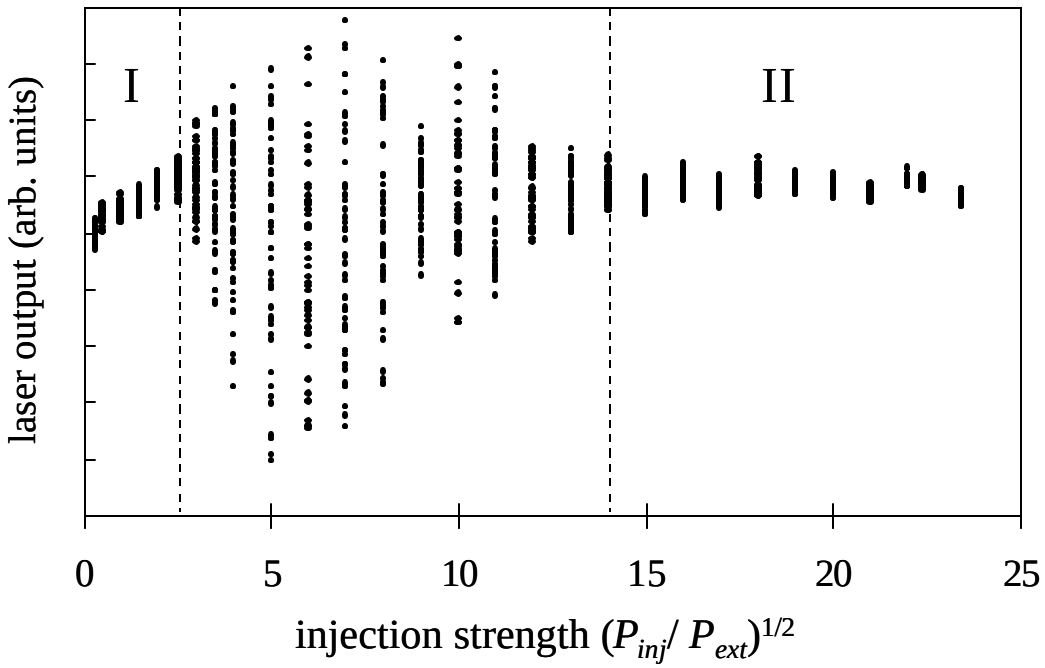

Fig.3 Bifurcation diagram of the slave laser output subject to periodic light injection as a function of injection strength.

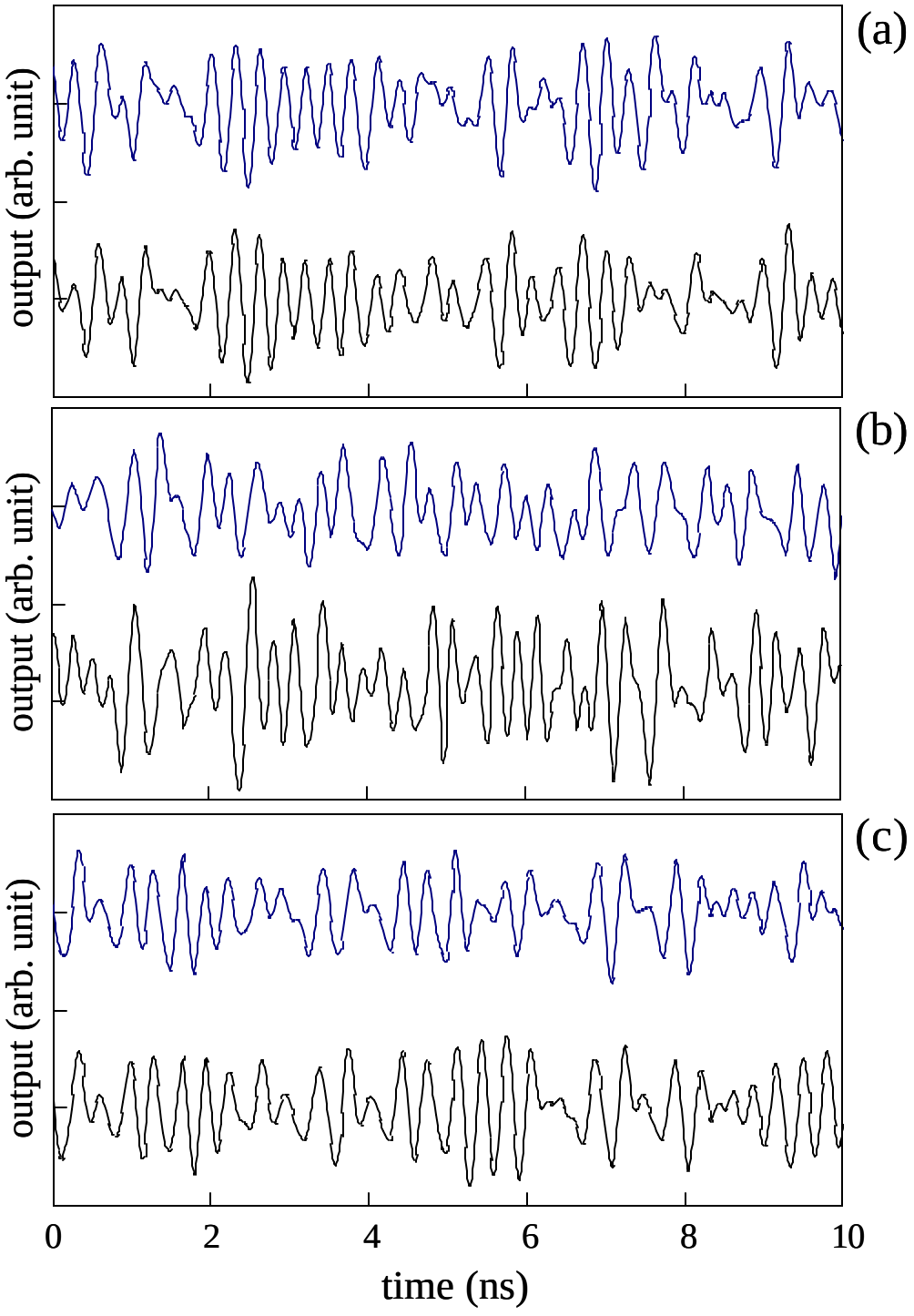

Fig.4 Slave laser outputs to chaotic injection signal. Upper trace: master output, lower trace: slave laser output. (a) $P_{inj} \approx P_{ext}$; (b) $P_{inj} \approx 10P_{ext}$; (c): $P_{inj} \approx 100P_{ext}$. In (a) and (c), the lower traces are properly shifted in time to match with the upper trace for the purpose of display.

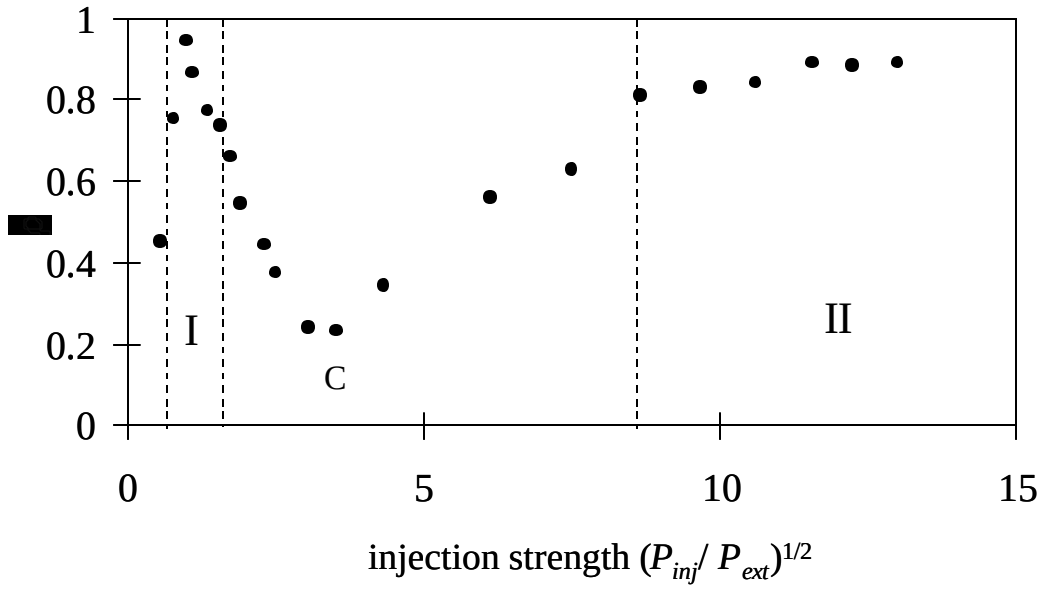

Fig. 5 Time lag versus the injection strength for chaotic injection signal.

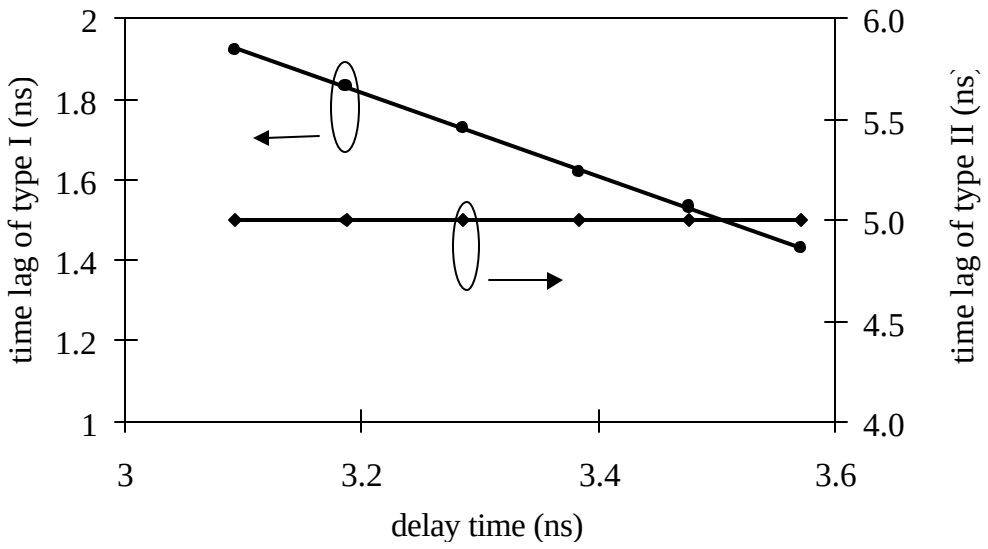

Fig.6 Time lag versus time delay measured at P_{inj}=P_{ext} for chaotic injection signal.

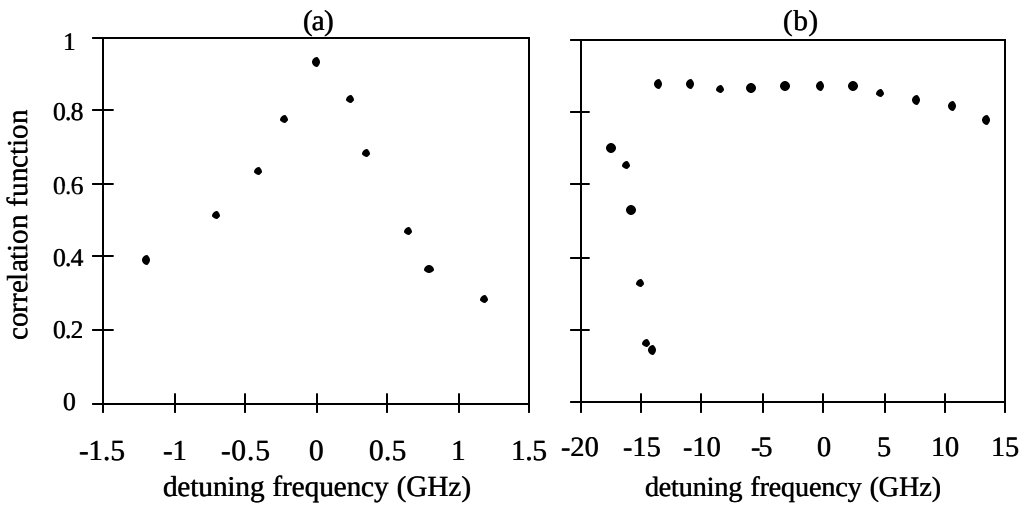

Fig.7 Correlation function versus frequency detuning at the injection level (a) P_{inj}=P_{ext} and (b) P_{inj}=125P_{ext} for chaotic injection signal.

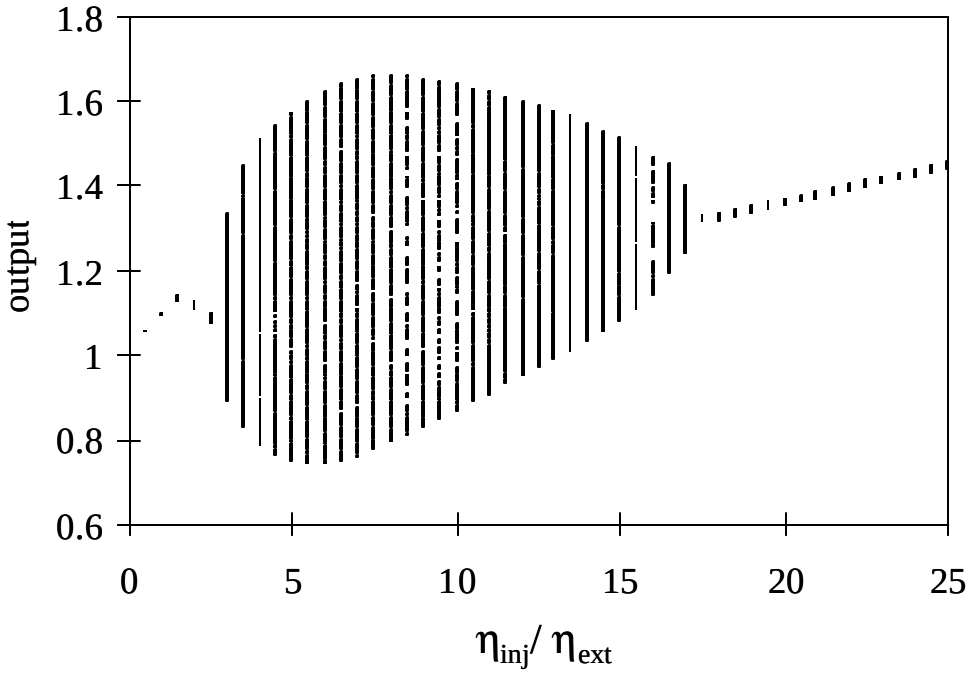

Fig.8 Numerical results of the bifurcation diagram of the slave laser output subject to periodic light injection.

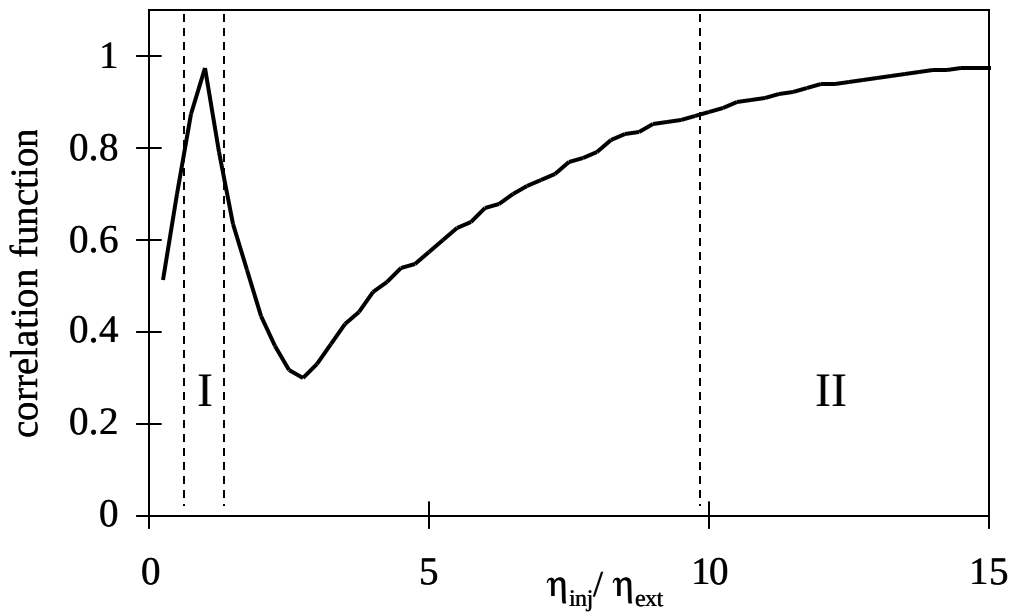

Fig.9 Numerical results of the correlation function versus the injection strength for chaotic injection signal.

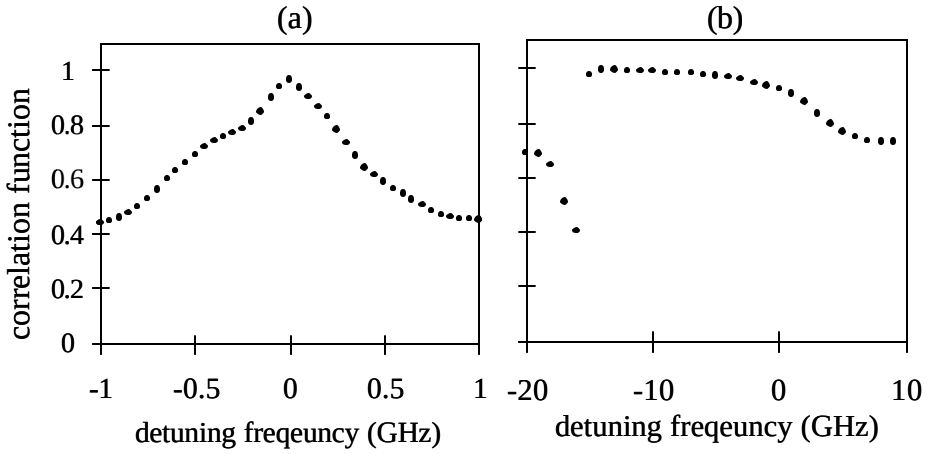

Fig.10 Dependencies of correlation on detuning frequency at injection level of (a) h_{inj}=h_{ext} and (b) h_{inj}=11.25h_{ext} for chaotic injection signal.

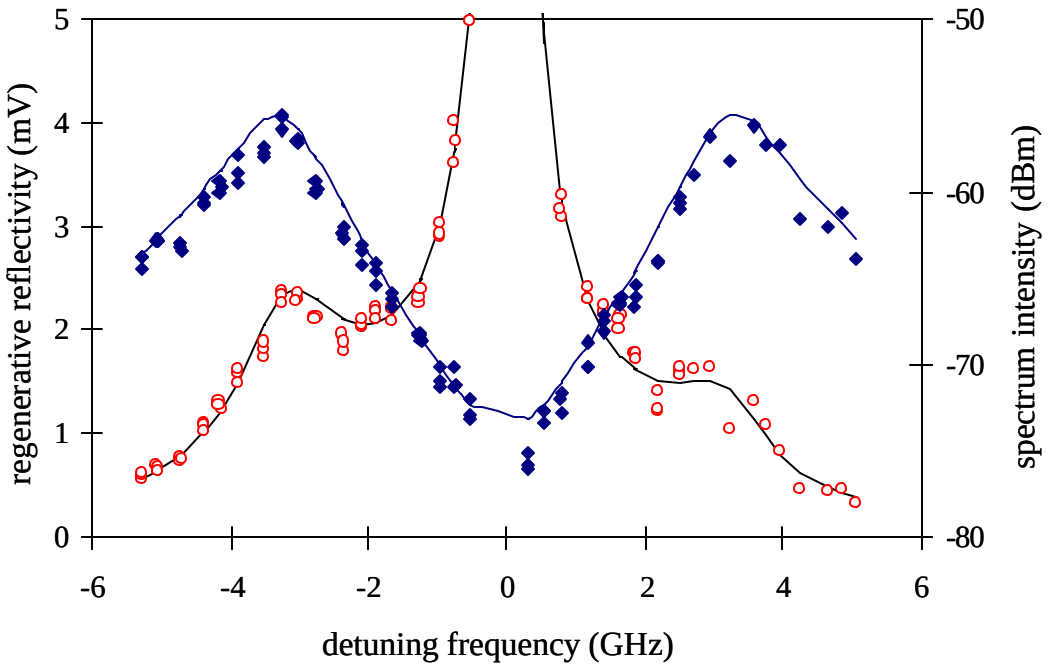

Fig. A-1 Spectra of regenerative reflectivity (left scale) and power spectrum (right scale) of the DFB laser subject to a weak optical injection. Circles: measured data; curves: fitting results using Eqs. (30) and (31) of Ref. [27].

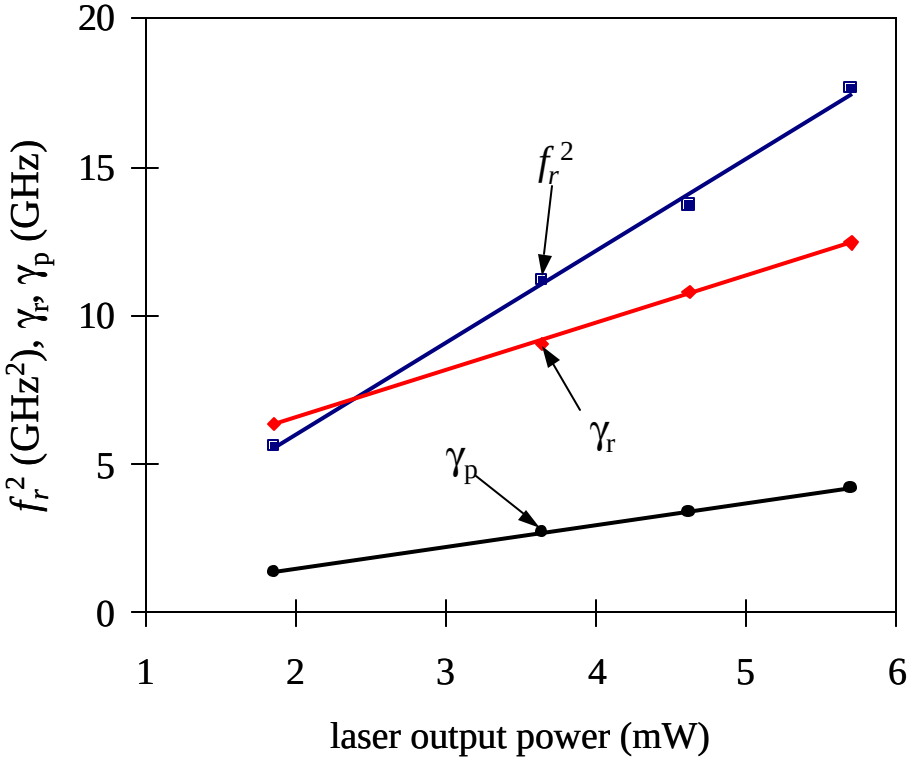

Fig. A-2 Power dependencies of g_r, g_p (unit: GHz), and f_r^2 (unit: GHz^2). Circles: measured data; lines: liner fitting.